

Two decades ammonium records from ice core in Qiangyong glacier in the Northern Himalayas

Ran Tian^{a,b}, Lide Tian^{a,b,c,d,*}



^a Institute of International Rivers and Eco-Security, Yunnan University, Kunming 650091, China
^b Yunnan Key Laboratory of International Rivers and Transboundary Eco-security, Kunming 650091, China
^c Key Laboratory of Tibetan Environment Changes and Land Surface Processes, Chinese Academy of Sciences, Institute of Tibetan Plateau Research, Beijing 100101, China
^d CAS Center for Excellence in Tibetan Plateau Earth Sciences, Chinese Academy of Sciences, Beijing 100101, China

ARTICLE INFO

Keywords:
 Glaciochemical record
 Ammonium
 Ice core
 South Asia
 Tibetan Plateau

ABSTRACT

The increase in anthropogenic emissions and associated climate change have become a growing critical environmental concern, with significant implications for human health and ecological security. The rapid economic growth in South Asia has contributed additional stress on the atmospheric environment in the surrounding regions. Earlier ice core chemical studies revealed a strong atmospheric transport to the Himalayan region from South Asia through the Indian summer monsoon. Continuous observation of atmosphere chemistry is not yet available, while ice core chemical record from high mountain regions can serve as an alternative proxy. So far, the influence of these transports on the southern Tibetan Plateau has not been adequately evaluated as only a few glaciochemical records are rebuilt. Here, we present a chemical record from a shallow ice core (with depth of 21.4 m), which was retrieved from the Qiangyong Glacier in the rain-shadow area of the Himalayas drilled in 2009 and dated back to the past 23 years of 1987–2009. The primary objective was to retrieve glaciochemical record and establish possible sources of soluble components, in particular those of NH_4^+ . Empirical orthogonal function (EOF) analysis on the eight major ions series (Ca^{2+} , Na^+ , Mg^{2+} , NH_4^+ , K^+ , Cl^- , NO_3^- , SO_4^{2-}) from this core reveals that NH_4^+ is loaded primarily separately on EOF3, likely suggesting a specific source out of the other ion signals. Both a back-trajectory model and the correlation analysis between NH_4^+ and SO_4^{2-} indicate the anthropogenic origin from South Asia. Although earlier ice core records showed a curbed increasing trend in NH_4^+ , our new data reveals that the increasing trend continued after 1980 and experienced a rapid increase after 2000. This trend is in accordance with the increasing population and agriculture activities in South Asia, corresponding with increasing anthropogenic emission. Spatial comparison of the Qiangyong ice core record with existing NH_4^+ records from other ice cores in the Tibetan Plateau show that concentrations of NH_4^+ are regionally increasing. However, the relatively small rise in Qiangyong record is probably in association with the effective transportation barrier of the Himalayas. This study advances the knowledge of atmospheric environmental change in the northern Himalayas and the air mass transport of anthropogenic pollutants from South Asia to the southern Tibetan Plateau via the summer Indian monsoon.

1. Introduction

Rapid economic growth and industrial and agricultural activities have contributed increasing pollutant emissions to the atmosphere since the 1850s, especially the 1930s (UNEP, 2012). Despite the actions of mitigation in North America and Europe, regulation of emissions had no significant effects in Asia, in particular South Asia, where emissions continue to rise (Akimoto, 2003; Krotkov et al., 2016). Distributions of anthropogenic aerosols are intricately linked to the climate system and hydrologic cycle (Al-Khashman, 2005; Kaufman et al., 2002) and are

largely driven by the pattern and strength of atmospheric circulation (Zhang et al., 2009, 2015). As the pollution pump and purifier of the world, the South Asian monsoon sustains a remarkably efficient cleansing mechanism, by which contaminants are deposited to the earth and some pollutants disperse globally in the upper troposphere, making air pollution in South Asia a source for regional and global climate benefits (Lelieveld et al., 2018). Atmospheric circulation brings masses, such as water vapor and aerosols, from South Asia to the Tibetan Plateau (TP) (Lüthi et al., 2014; Tian et al., 2001).

Ammonia is an important atmospheric component, with a short

* Corresponding author at: Institute of International Rivers and Eco-Security, Yunnan University, Kunming 650091, China.
 E-mail address: ldtian@ynu.edu.cn (L. Tian).

lifetime of 1–5 days or less and is easily neutralized by acid species converting to NH_4^+ aerosol without transporting over very long distances (Warneck, 1988). Anthropogenic sources of atmospheric ammonia include livestock wastes, fertilizers, and some industrial activities, while natural emissions would comprise only a minor part (Asman et al., 1998; Reis et al., 2009). The statistical atmospheric transport model TREND (Asman and Jaarsveld, 1992) indicated that emitted NH_3 returns to the surface mainly in the form of dry deposition of NH_3 and wet deposition of NH_4^+ , and that the contribution from NH_4^+ aerosol dominates the wet deposition of NH_x . Thus, ammonium deposited on a glacier surface during precipitation events can be preserved as a glaciochemical record in glacier ice.

High-resolution NH_4^+ records have been recovered from glaciers in various mountain regions of central Asia (Geng et al., 2007; Hou et al., 2003; Kang et al., 2002a; Kang et al., 2000; Qin et al., 2002; Thompson et al., 2000; Wake et al., 1993). These studies present a spatial and temporal variability of NH_4^+ in the TP, revealing past climate and environmental changes. The Himalayan region represents an ideal environment for studying the atmospheric composition, as the glaciochemical record contained in the Himalayan glaciers represents a valuable archive to reconstruct the history of the atmosphere (GRIP, 1993; Hou et al., 2003; Lelieveld et al., 2018; Tian et al., 2007; Wake et al., 1993). Due to the different pathways of atmospheric circulation and sources of ions in the Himalayas, glaciochemical records from the Himalayan ice cores show spatially devious records (Geng et al., 2007; Qin et al., 2002; Yang et al., 2012). Mt. Muztagata region is affected by the prevailing westerlies. East Rongbuk is under the Indian monsoon and the westerly jet. The NH_4^+ of the Muztagata is from the agricultural activity of Central Asia while the NH_4^+ of the East Rongbuk is associated with agricultural activity from South Asia. These ice core ammonium records show diverse trends during the period of their records (Hou et al., 2003; Zhao et al., 2008).

Here, we present a new glaciochemical record from Qiangyong ice core, which was drilled from the rain-shadow site of the Indian monsoon in the northern Himalayas in 2009. In particular, we focus on the ammonium record and assess possible sources and varying trends over approximately the past two decades during 1987–2009. We also studied the spatial differences in existing Himalayan ice core records from that region to help determine the impact of different seasonal precipitation patterns.

2. Study site and data

2.1. Study site

The Qiangyong Glacier is located between the Himalayan ranges and the Yarlung Zangbo River in the southern TP (Sun et al., 2016) (Fig. 1). The highest peak is Kaluxiong, with an altitude of 6674 m a.s.l. Melt water from the Qiangyong Glacier flows to Yamdrok-tso Lake, which is the largest inland lake in southern TP. The climate in the Himalayas is controlled by the southern branch of the westerlies from September through May and by the Indian monsoon from June to August (Tian et al., 2001, 2007). Additionally, the Indian monsoon precipitation determines the local precipitation level (Wake et al., 1993). However, since the Qiangyong Glacier is in the rain-shadow area of the Indian monsoon moisture transport, only strong monsoon activities can overcome the orographic barrier and bring precipitation there (Shrestha et al., 1997). Thus, this site has a strong monsoonal precipitation pattern. At the Langkazi meteorological station, 21 km away from the ice core drilling site, the average annual rainfall in summer (June to September) accounts for approximately 90% of the total annual precipitation (Sun et al., 2016; Tian et al., 2008), while little precipitation occurs in winter season.

The Qiangyong Glacier has a length of 4.9 km, a maximum width of 2.8 km and an area of 7.7 km² (Luo et al., 2003). The altitude of the glacier is between 5100 and 6674 m a.s.l. from terminus to its summit.

The glaciers in the region are slightly retreating in the recent decades, according to the remote sensing data (Ye et al., 2017).

2.2. Methodology

In April 2009, a 21.4 m shallow ice core with a diameter of 6.5 cm was retrieved at the accumulation zone of the Qiangyong Glacier (28.848°N; 90.221°E, 6070 m a.s.l.). An ice (firm) sample density was measured in situ during the ice core drilling for use in the glacier accumulation rate calculation. The ice core was frozen in a refrigerator for transportation and sent to the cold room in Lhasa for storage. There, the ice core was cut into 497 samples with an average interval of 5 cm on an ultra-clean cabin in a cold room. The outer 0.5 cm of each ice sample was scraped using a clean stainless-steel scalpel for stable oxygen isotope ratio measurements and the inner part was used for major ions analysis. The ice samples were put in polyethylene bottles, which had been pre-purified three times each. The ice samples were shipped to Beijing in a frozen state and melted before measurement.

The stable oxygen isotope ratio ($\delta^{18}\text{O}$) and chemical ions were measured in the Key Laboratory of Tibetan Environmental Changes and Land Surface Processes, Institute of Tibetan Plateau Research, Chinese Academy of Science. Stable water isotopes were measured via MAT-253 mass spectrometer, and the results were expressed as a relative deviation of heavy isotope content of Vienna Standard Mean Ocean Water (VSMOW). The measured precision is $\pm 0.15\%$ for $\delta^{18}\text{O}$. The cations (Ca^{2+} , Na^+ , Mg^{2+} , NH_4^+ , K^+) were measured by using a Dionex ion chromatograph, model ICS2000, with a CS12 4 mm column, 0.2 mL loop, and an isocratic 18 mM MAS eluent. The anion (Cl^- , NO_3^- , SO_4^{2-}) measurements were performed via the Dionex ion chromatograph, model ICS2500, with AS11-HC 4 mm column, 0.5 mL loop, and an isocratic 25 mM KOH eluent. The detection limits for the cation and anion measurements were below 1 ng g⁻¹.

The Langkazi meteorological station provided the daily meteorological data. The Southern Oscillation Index (SOI) was used in the analysis. SOI is usually considered as an index of the ENSO event to determine the sea level pressure differences between Tahiti and Darwin, Australia, and is calculated by the Australian Bureau of Meteorology (Ropelewski and Jones, 1987) (available at <http://www.bom.gov.au/climate/current/soihtm1.shtml>).

3. Ice core dating

$\delta^{18}\text{O}$ isotope values did not exhibit discernable annual variation due to insufficient winter accumulation, which also made seasonal isotope variations unapparent at the 5 cm sampling resolution. The similar result was explained by Pohjola et al. (2002) that large standard deviations in accumulation rates can blur the annual signal. Thus, the Qiangyong ice core was dated by utilizing high-resolution records of apparent seasonal variations of biogenic-source ions (NH_4^+ and NO_3^-) with dust-source (Ca^{2+} and Mg^{2+}), for well-preserved peaks of the ions due to the combination of dry and wet deposition (Fig. 2), and complemented by counting peaks in these ions (Joswiak et al., 2010). The dating result shows that this shallow ice core covered the time period from 1987 to 2009. For the incomplete annual records, the upper six samples for 2009 and the bottom for 1987 are not used in the annual calculation or discussion in this paper.

The ice core annual accumulation was retrieved by multiplying the length of each sample by its density, then was added up for each annual layer. The comparisons with annual precipitation data at the Langkazi station (Fig. 2) show coherent variation, with a coefficient of 0.82 (correlation significance at $p = .05$). However, the glacier accumulation rate is approximately 1.5 times of that at the low altitude precipitation at Langkazi, resulting from the vertical precipitation gradient in the Himalayan region (Cuo and Zhang, 2017; Xu et al., 2018). We also compared interannual ice core water isotope records with Southern Oscillation Index (SOI), a proxy of the interannual variation of large-

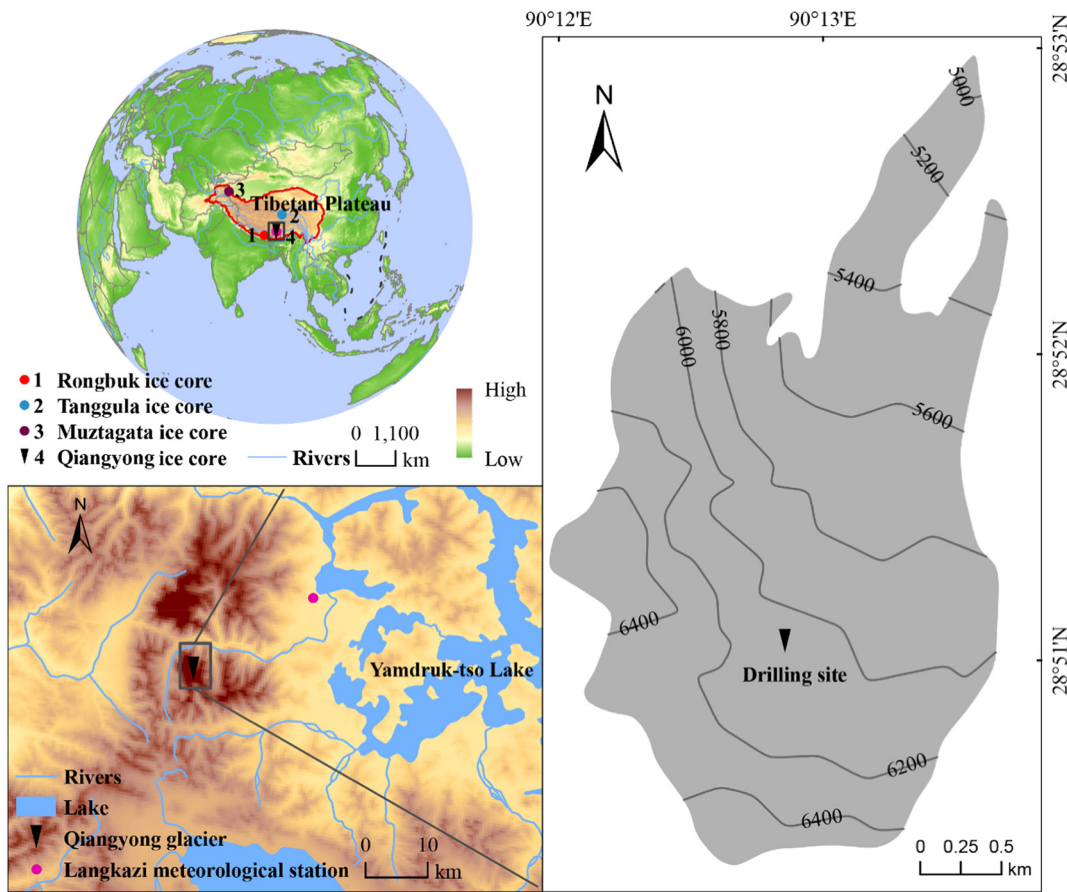


Fig. 1. Location of the Qiangyong Glacier and the ice core drilling sites.

scale atmospheric circulation, to further validate the dating results. The comparison is relied on the fact that the isotope in precipitation and ice core records over the Asia monsoon region is significantly related to El Niño-Southern Oscillation (ENSO) signal (Cai et al., 2017; Shao et al., 2017; Thompson et al., 2000). Dating uncertainty results from vague seasonal signals in some years due to the scarce winter season precipitation in the study region. The combination of dating techniques yields an annually resolved chronology that is accurate to within \pm one year of the core.

4. Results and discussion

4.1. The environmental information

4.1.1. $\delta^{18}\text{O}$ variation

Previous studies have found that the amount effect and temperature effect are dominant factors for the interannual variation of $\delta^{18}\text{O}$ in precipitation (Dansgaard, 1964; Siegenthaler and Oeschger, 1980; Tian et al., 2001; Yao et al., 1999). The precipitation amount effect is apparent in the southern TP precipitation isotope (Tian et al., 2003; Yao et al., 2013), while increasing consensus indicates that the annual variations of the precipitation isotope in the Asia monsoon are related to large-scale atmospheric circulation variations (Aggarwal et al., 2004; Cai and Tian, 2016; Vuille et al., 2005). The underlying mechanism suggested by the interannual variation of convection activity in the moisture source region is driven by the large-scale atmospheric circulation, in particular, ENSO events (Cai and Tian, 2016; Cai et al., 2017), and the interannual variability of the climate in almost all low-latitude regions (Rasmusson and Carpenter, 1982; Whetton and Rutherford, 1994).

The annual variations of $\delta^{18}\text{O}$ in another ice core, Qiangtang No.1

ice core, retrieved from the middle TP corresponds well with SOI and is potentially related to the convection intensity in the ocean source region (Shao et al., 2017), thereby implying the possible coherence in annual variation in ice core records in the large TP region. Fig. 3 presents the comparison of the annual $\delta^{18}\text{O}$ record of the Qiangyong ice core with SOI. The parallel variation indicates that the interannual variation of Qiangyong $\delta^{18}\text{O}$ is likely controlled by the large-scale atmospheric circulation, which is in agreement with the findings from other ice core isotope records (Cai et al., 2017; Shao et al., 2017; Thompson et al., 2000). This robust agreement also further constrained the dated result of this shallow ice core.

4.1.2. Environmental record

Fig. 4 presents the annual variations of major soluble ion (Ca^{2+} , Na^+ , Mg^{2+} , NH_4^+ , K^+ , Cl^- , NO_3^- , SO_4^{2-}) concentrations in the Qiangyong ice core. As a main feature, Ca^{2+} , Na^+ , Mg^{2+} , K^+ , Cl^- , SO_4^{2-} show coherent annual variations, indicating similar sources. During the two decades, the most notable peaks occurred in 1995 and 2003, while the average concentration in other periods remained at a relatively low level. Zheng et al. (2010) indicated that the maximum concentration in the ice core is in agreement with the strength of the dust storm, and the strength of the dust storm in 1995 is more powerful (Gou et al., 2012). Therefore, dust storm might be the most likely sources for the higher concentrations of ions. However, NH_4^+ and NO_3^- in ice core show different variation patterns from others. Fig. 4 also shows the variations of the annual mean value of NH_4^+ concentration during 1988–2008, from which we can see that the NH_4^+ level remains increasing during the two decades, with an annual increasing rate of $0.15 \mu\text{eq L}^{-1}\text{a}^{-1}$. Though weak drops can be observed at 1995/1996 and 2001/2002, the annual averaged NH_4^+ concentration during 2006–2008 ($4.14 \mu\text{eq L}^{-1}$) is 3.1 times of that in 1988–1990

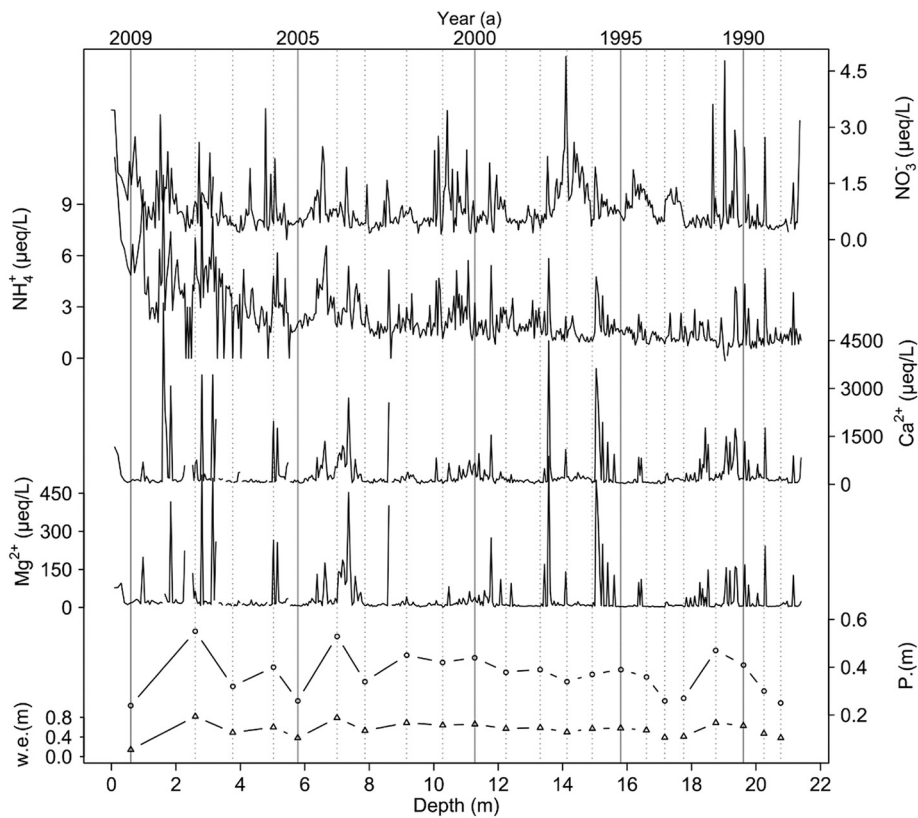


Fig. 2. Ice core dating with dotted and solid lines representing the annual layers of the Qiangyong ice core, together with the comparison of the ice core accumulation (Acc) rate (water equivalent depth) and annual precipitation (P) at Langkazi meteorological station.

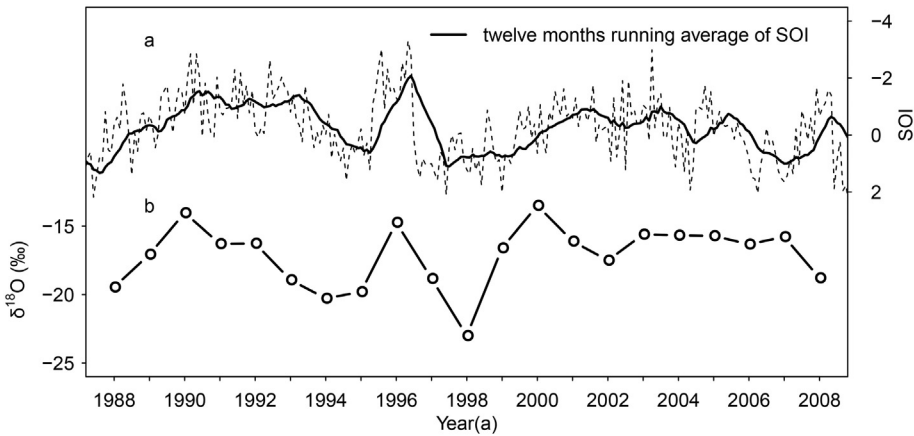


Fig. 3. Comparison of (a) monthly SOI (dotted line) and 12-month running average (solid line), and (b) the annual variations of the Qiangyong ice core $\delta^{18}\text{O}$ record.

($1.34 \mu\text{eqL}^{-1}$), of which the comparison is far more evident for increasing trend than other periods.

4.2. Sources assessment

4.2.1. Multivariate empirical orthogonal function (EOF) analysis and correlation analysis

Multivariate empirical orthogonal function (EOF) analysis is a statistical method describing the prime field in an all-round way and analysing the structure of the time-series of the prime field. It is suitable for detecting a common structure within multiple records, and this technique is less sensitive to small dating errors introduced by the ice core series (Meeker et al., 1997). We performed EOF analysis on the time series of the eight major ions (Ca^{2+} , Na^+ , Mg^{2+} , NH_4^+ , K^+ , Cl^- ,

SO_4^{2-} and NO_3^-), and the results are summarized in Table 1. EOF 1, explains 65% of the total variance of the major ion series. All major ions (except NO_3^- and NH_4^+) are strongly loaded on EOF1 and are significantly correlated (Fig. 5). The result is in accordance with published glaciochemical results from the study region (Wake et al., 1993), which show that major ions are the mineral aerosol input from the large desert basin, indicating that the dust is the primary source. In addition, the ion concentration sequence $\text{Ca}^{2+} > \text{Na}^+ > \text{Mg}^{2+} > \text{K}^+$ is in agreement with that in the earth (Zhang et al., 2009). Wake et al. (1993) reported that Na^+ and Cl^- in southeastern TP are indicative of the mineral aerosol input. The average value of $\text{Na}^+:\text{Cl}^-$ ratio of each Qiangyong ice sample is 1.15, and the ratio of $\text{Na}^+:\text{Cl}^-$ in the snow sample is 1.41 ± 0.4 , which reflects inputs of Na^+ rich material (Wake et al., 1992). Thus, sea-salt contributions to ions in the Qiangyong ice core are

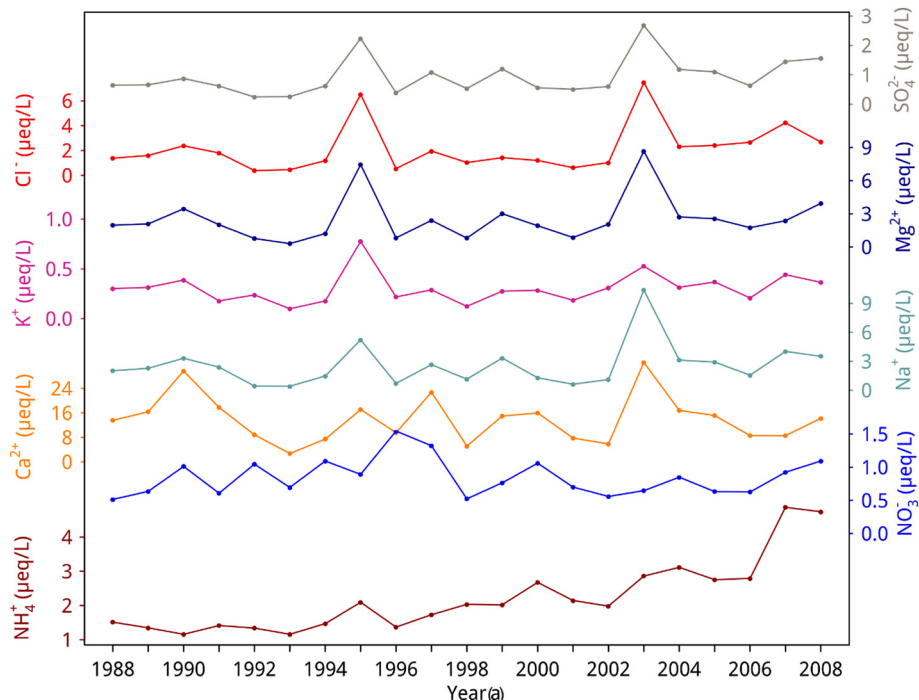


Fig. 4. Annual variations of major soluble ions in the Qiangyong ice core.

Table 1

EOF associations for the time series of the major ions preserved in the Qiangyong ice core.

	EOF1	EOF2	EOF3
Na ⁺	0.96	-0.02	-0.11
Mg ²⁺	0.97	0.04	-0.13
Ca ²⁺	0.72	0.45	-0.31
K ⁺	0.88	0.06	0.07
Cl ⁻	0.96	-0.11	0.00
NH ₄ ⁺	0.45	-0.46	0.72
NO ₃ ⁻	-0.04	0.80	0.59
SO ₄ ²⁻	0.98	-0.06	0.09
Total	0.65	0.14	0.12

negligible. The ratio approaches that of halite (1.0), and the loose deposits characterized by fine grain are widely distributed in the valley of Qiangyong Glacier Basin (Sun et al., 2016). Then, possible sources for Na⁺ and Cl⁻ are the evaporite deposits from regional salt lakes (Hou et al., 2003). Sources of NO₃⁻ are complex, including soil process, biogenic activity, anthropogenic activity such as the use of fertilizers and transported via from the stratosphere (Legrand and Delmas, 1986; Mayewski et al., 1983; Russell and McGregor, 2010). NO₃⁻, dominating EOF2, may be indicative of sources of lightning in middle-low latitudes (Sheng et al., 1996) and anthropogenic activities including fossils fuels burning and biomass burning (Schumann and Huntrieser, 2007). On EOF3, NH₄⁺ is loaded, probably indicating a consequence of a biogenic source from agricultural activities.

Fig. 5 presents the correlation analysis of the inter-annual concentration of major soluble ions in the Qiangyong ice core. The values of correlation coefficients are calculated from the individual sample data of the ice core (The correlation is significant at the 0.05 level). As a main feature, most of the soluble ions are significantly correlated ($p < .05$) because of the strong seasonal variability (Zheng et al., 2010). The significant correlations among the soluble ions, indicate a similar transmission or sedimentation process, rather than the same emission source strength. The high correlation coefficients among Ca²⁺, Na⁺, Mg²⁺, K⁺, SO₄²⁻ and Cl⁻, indicate that the ions originated mainly from mineral dust particles., While, the correlation coefficients

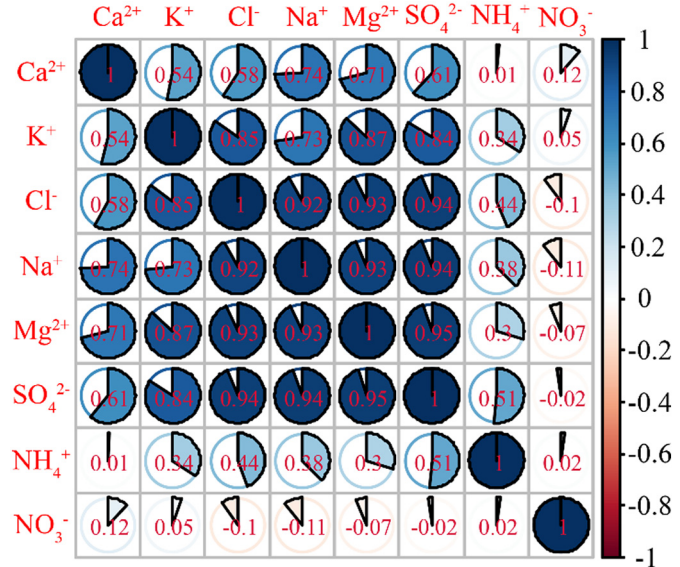


Fig. 5. Correlation analysis of eight major soluble ions (Ca²⁺, Na⁺, Mg²⁺, NH₄⁺, K⁺, Cl⁻, SO₄²⁻ and NO₃⁻) of the Qiangyong ice core. The different colours in the colour bar represent the strength of the correlation. Colours range from deep red to dark blue, representing varying degrees of the correlation coefficient. The colour red means that the correlation coefficient is -1 and the blue stands for 1. The correlation coefficients are also shown in the circle in the graph, and values in the circle are calculated from the individual sample data of the ice core (Bold font indicates that the correlation is significant at the 0.05 level). (For interpretation of the references to colour in this figure legend, the reader is referred to the web version of this article.)

between NO₃⁻ and major mineral dust ions (Ca²⁺, Na⁺, Mg²⁺, K⁺, SO₄²⁻ and Cl⁻) are not statistically significant, suggesting a specific source of NO₃⁻ in this area. The result is in accordance with the EOF analysis.

4.2.2. Back trajectory analysis

The HYbrid Single-Particle Lagrangian Integrated Trajectory model (HYSPPLIT_4) (Stein et al., 2015; Rolph et al., 2017) was used to track the direction of the air parcels carried by the circulation, predict the wind field situation in time and analyse the precipitation with the circulation path (Draxler and Hess, 1998), and was also used to calculate the physical process of particle transport with air masses. To determine the seasonal origin of air masses and establish source-receptor relationships for the Qiangyong ice core record, we used HYSPPLIT_4 to calculate the 5-day atmospheric backward trajectories reaching the ice core drilling site (The data is from <ftp://arlftp.arlhq.noaa.gov/pub/archives/gdas1>) (Stein et al., 2015) during the year of 2005. Meteorological field data is divided into four time-groups a day: 00:00, 06:00, 12:00, and 18:00 UTC, with $2.5^\circ \times 2.5^\circ$ horizontal resolution. We set one vertical layer at 1000 m above ground level (AGL). The calculation heights were fixed at 500, 1000, and 1500 m above the ground (Barbaro et al., 2015; Zhang et al., 2009; Dvorská et al., 2009). The choice of 1000 m AGL as the trajectory endpoint ensures that the trajectory starts in the atmospheric boundary layer (Dvorská et al., 2009). Also, the turbulent mixed fully in the Ekman layer and Ekman pumping is strongest in the top of the Ekman layer. Therefore, to ensure the condition is well mixed and no local effect in the atmospheric surface layer, starting height lower than 1000 m was excluded from the analysis. The pollutant sources are mainly in the Ekman layer, starting height above this layer was also excluded from the analysis. A cluster analysis was performed for the monthly calculated trajectories, and the results are shown in Fig. 6. The back-trajectory analysis shows an apparent seasonal shift of the prevailing wind in monsoon (June–September) season and non-monsoon season (October–May). In non-monsoon season, a persistent westerly jet characterized the atmospheric circulation pattern. The back-trajectory results show that most of the aerosols likely originated from the Middle East and south of the Caspian Sea, passing through Iran, Afghanistan, Pakistan, India, and Nepal. In monsoon season, a strong wind branching from the south to the central Himalayas characterized the atmospheric circulation pattern. The air mass originates from the Bay of Bengal, passes through India, Nepal and arrives at the Himalayas. Therefore, it is very likely that the NH_4^+ aerosol source preserved in the Qiangyong ice core is from South Asia.

4.2.3. Relationship between ammonia record and temperature change

A previous study showed that ammonia emissions from the regional ecosystem are supposed to be enhanced by global warming (Asman et al., 1998; Bouwman et al., 1997). Agriculture-originated ammonia was believed to be the primary source of NH_4^+ in ice core records (Hou et al., 2003; Qin et al., 2002), and the agricultural activities, which are intensive in summer, augment the seasonal NH_4^+ variations (Goebes et al., 2003). To access the possible driver of the increase in ammonium concentration in the study region during recent years, we made a comparison among the annual ammonium concentration, the Northern Hemisphere temperature anomaly (Jones et al., 2010) (The data is available at <https://crudata.uea.ac.uk/cru/data/temperature>) and the local meteorological station air temperature change (Fig. 7).

Similar trends exist between the NH_4^+ concentration and the air temperature during the overlapping period. We found correlation coefficients of $r = 0.47$ ($p < .05$) for the local temperature and $r = 0.71$ ($p < .05$) for the northern Hemisphere temperature anomaly. Higher temperature may increase NH_3 emissions from the breakdown of animal excreta and dead plant in soil by ammonification (Kang et al., 2002b). Soil can also release more nitrogen compounds under a rapidly warming environment (Butler et al., 2012), thus contributing significantly to the total amounts of atmospheric NH_3 .

4.2.4. Anthropogenic influence on ammonia record and potential sources

The increasing ammonia concentration in the Qiangyong ice core probably reflects the increasing emission in the source regions. Globally, agriculture represents the largest source of atmospheric NH_3 ,

and more than half of global atmospheric NH_3 is emitted from livestock and crops (Sutton et al., 2013). Domestic animals are the largest source of atmospheric NH_3 , comprising a combined ~40% of natural and anthropogenic emissions, while synthetic fertilizers and agricultural crops together account for ~23% of total emissions (Warneck, 1988). The most significant emission from livestock is from cattle, followed by pigs (Yamaji et al., 2004). In addition, the use of urea and ammonium bicarbonate and the cultivation of rice have led to a high average NH_3 loss rate from chemical N fertilizer in South Asia (Yan et al., 2003). However, there is no evidence supporting a local anthropogenic source for ammonia near Qiangyong. Tibet is a low-populated region, with a growth rate of only 0.44%. In addition, an earlier study suggested that the ammonium concentrations in snow above 5600 m a.s.l. are only slightly affected by local anthropogenic or biogenic sources (Ikegami et al., 2009), while the Qiangyong ice core was retrieved from 6070 m a.s.l.

Therefore, we compared the NH_4^+ record of the ice core with the factors related to emission in South Asia. Data on the direct observation of the ammonia emission time series are unavailable in our study region. Hence, we used statistics related to all these major factors and the population of the India and Nepal retrieved from the Food and Agriculture Organization of the United Nations (FAO) (<http://www.fao.org/statistics/databases/zh/>). These data show accelerating anthropogenic activity (Fig. 8). Fertilizer application is associated with NH_3 volatilization (Kang et al., 2002b), and synthetic fertilizer application cause more NH_3 volatilization. In Fig. 8, the amount of fertilizer application shows an increasing trend, with an exception only in 2002. This increasing trend is roughly parallel with the increasing trend in NH_4^+ record (Fig. 4). Both the population growth during the period and increasing trend in rice production during 2002–2009, matches the trend of the NH_4^+ record in the Qiangyong ice core. Though the number of livestock (i.e., cattle and pig) does not show an increasing trend, the overall current number of livestock is at a level that suggests a high NH_3 emission. Therefore, almost all of the factors suggest an increasing trend of agriculture-associated NH_3 emission, which is likely to contribute to the increasing NH_4^+ concentration in the Qiangyong ice core.

4.3. Spatial variations of glacier ammonia records

A few ice core chemical records in the TP allow for a discussion of the spatial characteristics of NH_4^+ variations. Then we evaluated the spatial difference of the NH_4^+ records in four different ice cores. In Fig. 9, we compared our NH_4^+ record with the chemical data from East Rongbuk ice core drilled at 6500 m a.s.l. (Hou et al., 2003; Kang et al., 2002a; Qin et al., 2002), Muztagata ice core drilled at the elevation of 7010 m a.s.l. (Zhao et al., 2008) and Tanggula ice core drilled on the saddle between the two Tanggula summits at 5746 m a.s.l. (Zheng et al., 2010). The four ice cores are located in different geophysical locations with varying atmospheric controls. The East Rongbuk Glacier is located in Mount Qomolangma, with a summer type glacier accumulation (Liu et al., 2010; Wang et al., 2013), while the Qiangyong Glacier is located between the Himalayan ranges and the Yarlung Zangbo River, where the atmospheric circulation is dominated by the Indian monsoon in summer and the westerly jet in winter. The Tanggula Glacier is located in the central TP, within the transition zone from an arid and semi-arid continental climate to a warm and moist marine climate (Tian et al., 2001). And Mt. Muztagata is located on the East Pamir Plateau in Central Asia, affected by the prevailing westerlies (Fig. 1).

The NH_4^+ concentration in the East Rongbuk ice core (for comparison we chose part of the East Rongbuk ice core data from 1940 to 1998) shows substantially increasing trend, reflecting the growing regional agricultural activities in South Asia and the relationship with atmospheric circulation (Kang et al., 2002a; Qin et al., 2002). However, this increasing trend has curbed after 1980 and then become stable, with a slight decreasing trend. Under the coherent large-scale

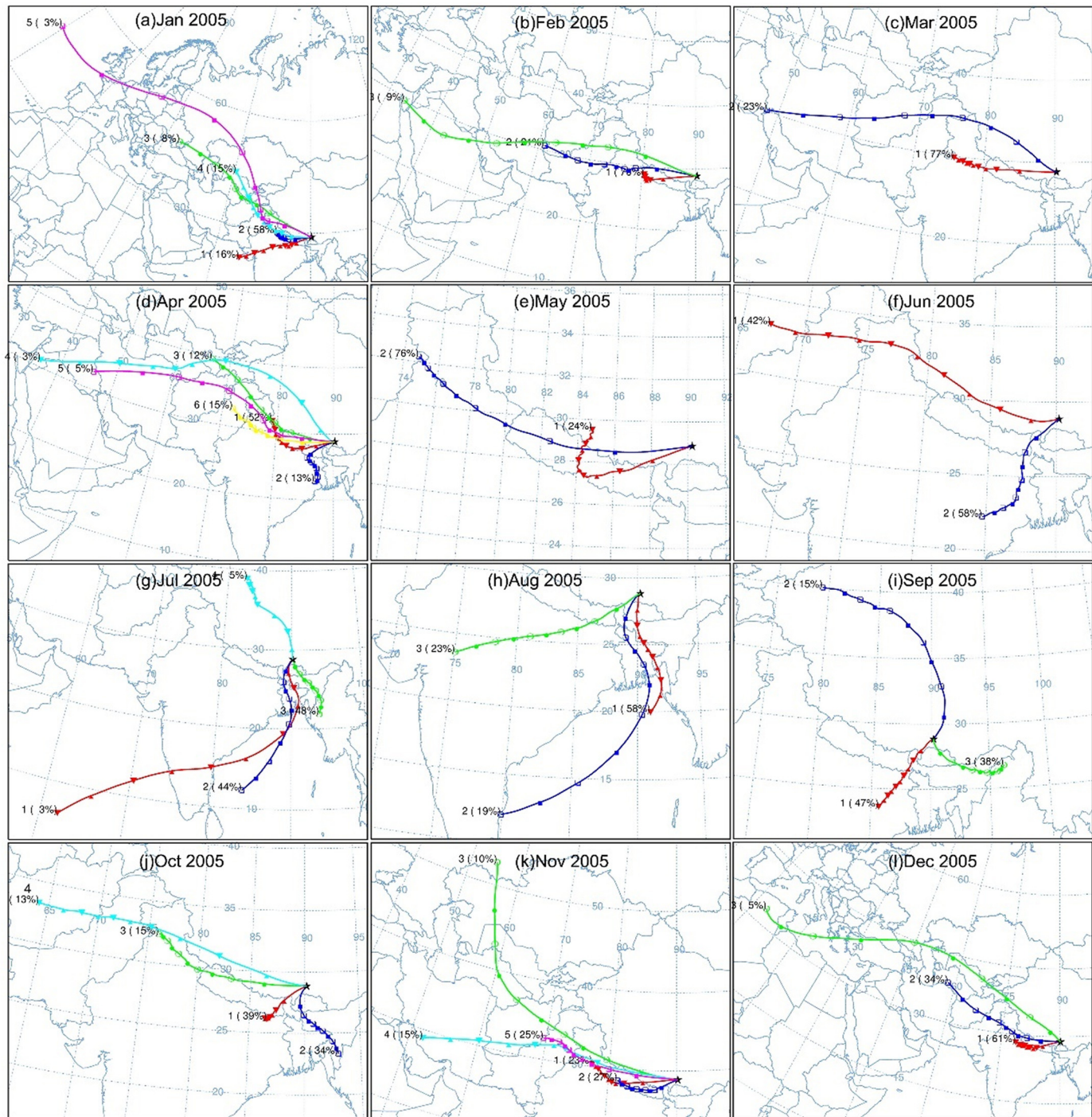


Fig. 6. The cluster analysis of the monthly atmospheric back trajectories with HYSPLIT calculated for the year 2005 in the ice core drilling site: (a) January (b) February (c) March (d) April (e) May (f) June (g) July (h) August (i) September (j) October (k) November (l) December. The single digit numbers are cluster identifiers. The percentage of contribution for each cluster is listed in brackets.

circulation and unanimous source, NH_4^+ showed a similar trend in both the East Rongbuk ice core and the Qiangyong ice core during the period of their records. The increasing trend of NH_4^+ concentration after the 1990s in Qiangyong ice core, also hints a sustained increasing trend of ammonia emission in the source region. The profiles of NH_4^+ concentration from Muztagata also displayed a rising trend after 1940 but peaked in the late 1990s, out of phase with East Rongbuk record. Subjected to the control of westerlies, Mt. Muztagata is affected by emissions in Central Asia regions (Zhao et al., 2008). However, compared with ice core records from the northern and southern periphery

of the TP, lower anthropogenic contributions are recorded in the Tanggula ice core. The NH_4^+ of Tanggula ice core is mainly influenced by soil and biogenic emissions, and exhibit comparable trends to the temperature anomaly, with a near simultaneous increase in the early 1980s (Zheng et al., 2010).

For the similar source, we only compared the annual average of NH_4^+ recorded in the two ice cores in Himalayas as spatial diversity and discussed possible reasons for the spatial setting (Fig. 9). The average NH_4^+ in the East Rongbuk ice core during the period from 1989 to 1997 is $4.44 \mu\text{eq/L}$, while the corresponding NH_4^+ in the

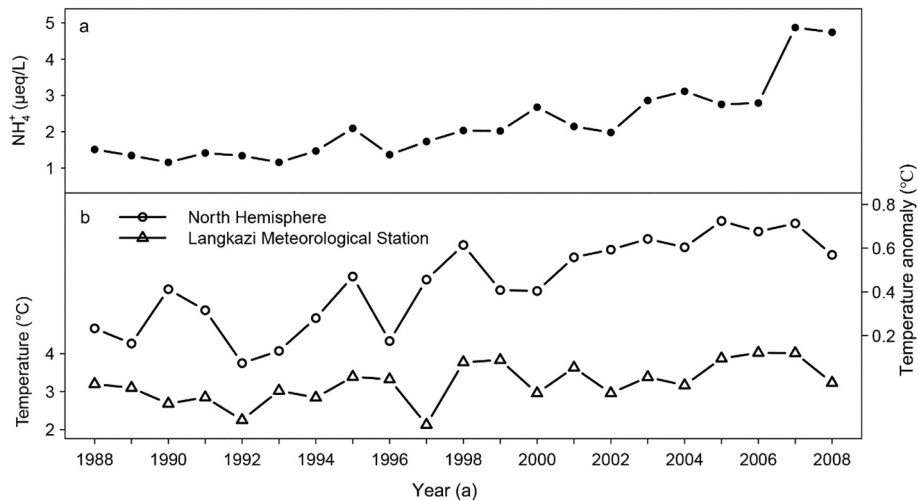


Fig. 7. Comparison of the annual mean of NH_4^+ concentration with temperature anomalies from the Northern Hemisphere and temperature records from the Langkazi Meteorological Station during 1988–2008.

Qiangyong ice core is 1.48 $\mu\text{eq/L}$. One possible reason for the difference is that the East Rongbuk Glacier is located on the top of Himalayas and directly faces the summer Indian monsoon transport, while the Qiangyong ice core is located in the rain-shadow area of the Himalayas. Due to the effective barrier of the Himalayas against the ammonium transport to the inland of the TP, the level of NH_4^+ in the ice core on the southern slope is higher than that on the northern slopes of the Himalayas (Geng et al., 2007), which the crucial reason is the difference in seasonality in glacier accumulation and NH_4^+ deposition. Also, the NH_4^+ was preferentially washed out in the precipitation events while

passing over the Himalayas, and possibly lowered the NH_4^+ in the subsequent precipitation as in Qiangyong glacier in the northern Himalayas. Meteorological effects cause seasonal variations, and the highest concentration of NH_4^+ occur during spring, while the lowest values occur in late summer (Geng et al., 2007; Kang et al., 2000). The Qiangyong glacier receives most of its accumulation during the summer monsoon season. Therefore, NH_4^+ record has the lowest annual average due to the lack of winter and spring precipitation. The seasonal accumulation variations may partly explain the lower concentration of NH_4^+ in the Qiangyong ice core.

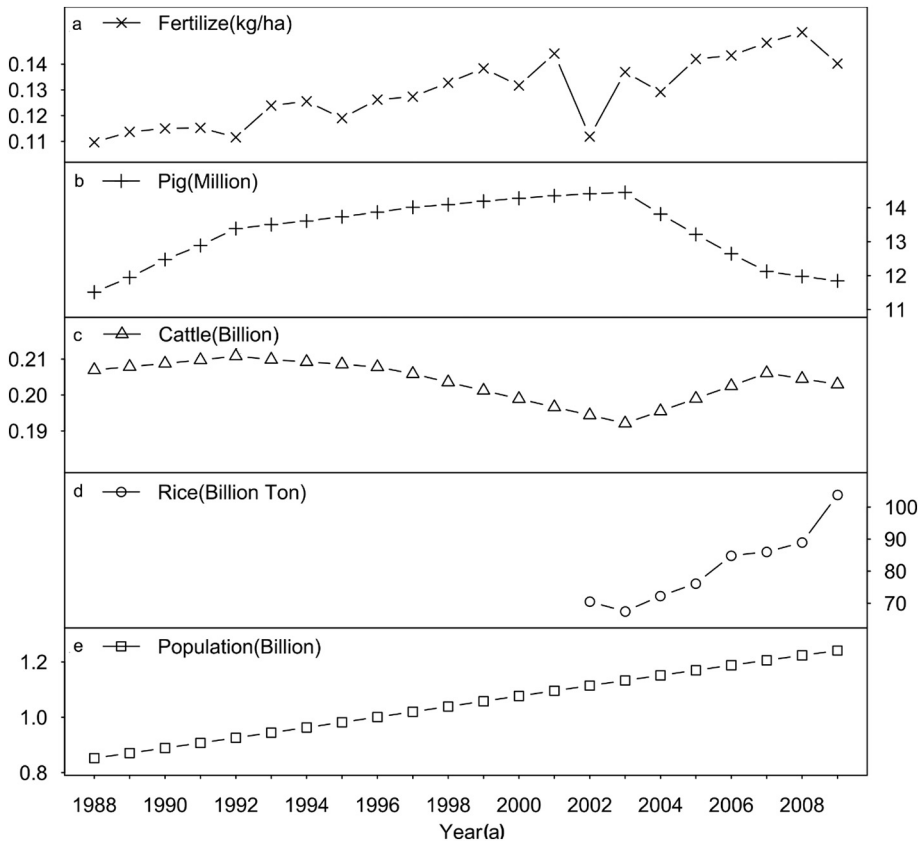


Fig. 8. Trends of factors that contribute to ammonia emission: (a) fertilizer (kg/ha); (b) pig (million); (c) cattle (billion); (d) rice (billion ton); (e) population (billion) in India and Nepal for the period of 1988–2009.

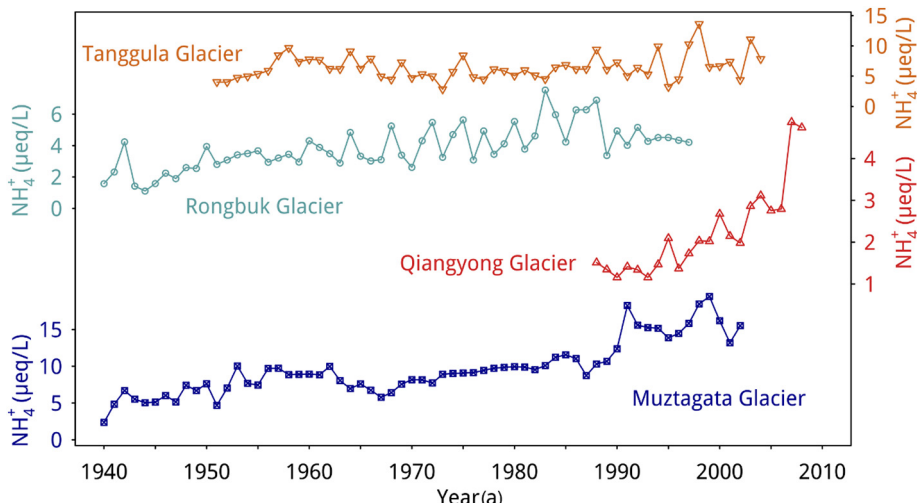


Fig. 9. Annual NH_4^+ average of the Qiangyong ice core (1988–2008), in comparisons with the ice core NH_4^+ record from the East Rongbuk Glacier from Hou et al. (2003), the Mt. Muztagata (Zhao et al., 2008) and the Mt. Tanggula (Zheng et al., 2010).

Therefore, the observed differences in NH_4^+ variations in ice cores for these geographic regions may be triggered by the regional differences in emission source strength and the effect of specific geographical location on the deposition for NHx ($\text{NH}_3 + \text{NH}_4^+$).

The result from our new ice core analysis showed a continuous increasing trend of NH_4^+ concentration during the observation period of 1988–2008. However, we acknowledge that the time covered by this shallow ice core is still short and also for the most recent record of data. Consequently, a new, longer ice core from this glacier will provide a longer and newer record.

5. Conclusion

We present a new glaciochemical record from the Qiangyong shallow ice core in the northern Himalayas, covering the atmospheric environment record of 1987–2009. The data have expanded the knowledge of the spatial and temporal glaciochemical substances in the Himalayas and the anthropogenic mass transportation from South Asia to the inside of the TP through the summer Indian monsoon.

Multivariate empirical orthogonal function (EOF) analysis and the correlation analysis shows that all major ions (except NO_3^- and NH_4^+) are strongly loaded on EOF1 and are significantly correlated, indicating that the major ions are the mineral aerosol input from the large desert basin, and the dust is the primary source. NH_4^+ is loaded mainly on EOF3 and shows a weak correlation with other ions, indicating a specific biogenic source from the agricultural activities.

The constant increasing NH_4^+ trend in the ice core, together with the back-trajectory analysis, shows that the NH_4^+ aerosol source is from South Asia. The enhancement of NH_3 emission suggests that the agriculture activities in South Asia, especially the economic growth (population, crop, fertilizer, and livestock) of India and Nepal, are responsible for the increasing emission.

The comparison with other ice core glaciochemical records suggests a continuously increasing trend in NH_3 emission and that the vast Himalayan range may block the NH_4^+ transportation to the inland plateau. A more crucial reason for the difference is from the seasonality of precipitation and NH_4^+ deposition on the two sides of the Himalayas. We confirm that the regional differences in atmospheric circulation patterns and geographical features may result in the different spatial distribution pattern of the glaciochemical record between the southern and northern slopes of the Himalayas.

Acknowledgements

This research was partially supported by the National Nature Science Foundation of China (Grant Nos. 41530748, 41771043). We also gratefully acknowledge the NCEP/NCAR and the National Meteorological Center of the Chinese Meteorological Association (CMA) for the meteorological data used in this research. We are grateful to all members of the Qiangyong Expedition in 2009 for their support in drilling the ice core.

References

- Aggarwal, P.K., Fröhlich, K., Kulkarni, K.M., Gourcy, L.L., 2004. Stable isotope evidence for moisture sources in the Asian summer monsoon under present and past climate regimes. *Geophys. Res. Lett.* 31, L08023. <https://doi.org/10.1029/2004GL019911>.
- Akimoto, H., 2003. Global air quality and pollution. *Science* 302, 1716–1719. <https://doi.org/10.1126/science.1092666>.
- Al-Khashman, O.A., 2005. Ionic composition of wet precipitation in the Petra Region, Jordan. *Atmos. Res.* 78, 1–12. <https://doi.org/10.1016/j.atmosres.2005.02.003>.
- Asman, W.A.H., Jaarsveld, H.A.V., 1992. A variable-resolution transport model applied for NH_3 in Europe. *Atmos. Environ.* 26, 445–464. [https://doi.org/10.1016/0960-1686\(92\)90329-J](https://doi.org/10.1016/0960-1686(92)90329-J).
- Asman, W.A.H., Sutton, M., Schjorring, J., 1998. Ammonia: emission, atmospheric transport and deposition. *New Phytol.* 139, 27–48. <https://doi.org/10.1046/j.1469-8137.1998.00180.x>.
- Barbaro, E., Zangrando, R., Vecchiato, M., Piazza, R., Cairns, W.R.L., Capodaglio, G., Barbante, C., Gambaro, A., 2015. Free amino acids in Antarctic aerosol: potential markers for the evolution and fate of marine aerosol. *Atmos. Chem. Phys.* 15, 5457–5469. <https://doi.org/10.5194/acp-15-5457-2015>.
- Bouwman, A.F., Lee, D.S., Asman, W.A.H., Dentener, F.J., Van, D.H., W, K., Olivier, J.G.J., 1997. A global high-resolution emission inventory for ammonia. *Glob. Biogeochem. Cy.* 11, 561–587. <https://doi.org/10.1029/97GB02266>.
- Butler, S.M., Melillo, J.M., Johnson, J.E., Mohan, J., Steudler, P.A., Lux, H., Burrows, E., Smith, R.M., Vario, C.L., Scott, L., Hill, T.D., Aponte, N., Bowles, F., 2012. Soil warming alters nitrogen cycling in a New England forest: implications for ecosystem function and structure. *Oecologia* 168, 819–828. <https://doi.org/10.1007/s00442-011-2133-7>.
- Cai, Z.Y., Tian, L.D., 2016. Atmospheric controls on seasonal and interannual variations in the precipitation isotope in the East Asian Monsoon region. *J. Clim.* 29, 1339–1352. <https://doi.org/10.1175/JCLI-D-15-0363.1>.
- Cai, Z.Y., Tian, L.D., Bowen, G.J., 2017. ENSO variability reflected in precipitation oxygen isotopes across the Asian Summer Monsoon region. *Earth. Planet. Sc. Lett.* 475, 25–33. <https://doi.org/10.1016/j.epsl.2017.06.035>.
- Cuo, L., Zhang, Y.X., 2017. Spatial patterns of wet season precipitation vertical gradients on the Tibetan Plateau and the surroundings. *Sci. Rep.* 7, 5057–5066. <https://doi.org/10.1038/s41598-017-05345-6>.
- Dansgaard, W., 1964. Stable Isotopes in Precipitation. *Tellus* 16, 436–468. <https://doi.org/10.3402/tellusa.v16i4.8993>.
- Draxler, R.R., Hess, G.D., 1998. An overview of the HYSPLIT.4 modelling system for trajectories. *Aust. Meteorol. Mag.* 47, 295–308 FAOSTAT, [http://data.fao.org/dataset-data-filter?entryId=f25df775-e5da-4170-bc16-ef4ec030144f&tab=data_\(2014\)](http://data.fao.org/dataset-data-filter?entryId=f25df775-e5da-4170-bc16-ef4ec030144f&tab=data_(2014)).
- Dvorská, A., Lammel, G., Holoubek, I., 2009. Recent trends of persistent organic pollutants in air in Central Europe – air monitoring in combination with air mass trajectory

- statistics as a tool to study the effectivity of regional chemical policy. *Atmos. Environ.* 43, 1280–1287. <https://doi.org/10.1016/j.atmosenv.2008.11.028>.
- Geng, Z.X., Hou, S.G., Zhang, D.Q., Kang, S.C., Wang, Y.T., Liu, Y.P., 2007. Major ions in Ice Cores and Snowpits from the Himalayas: temporal and spatial variations and their sources. *J. Glaciol. Geocryol.* 29, 191–200. <https://doi.org/10.1631/jzus.2007.A1858>.
- Goebes, M.D., Strader, R., Davidson, C., 2003. An ammonia emission inventory for fertilizer application in the United States. *Atmos. Environ.* 37, 2539–2550. [https://doi.org/10.1016/S1352-2310\(03\)00129-8](https://doi.org/10.1016/S1352-2310(03)00129-8).
- Gou, S.W., Wu, Y.Q., Xia, D.D., Pan, J., 2012. Spatiotemporal distribution characteristics and circulation background of sandstorm occurrence frequency in Qinghai-Tibet Plateau in winter and spring. *J. Nat. Disasters* 5, 135–143. <https://doi.org/10.1007/s11783-011-0280-z>.
- GRIP, 1993. Climate instability during the last interglacial period recorded in the GRIP ice core. *Nature* 364, 203–207. <https://doi.org/10.1038/364203a0>.
- Hou, S.G., Qin, D.H., Zhang, D.Q., Kang, S.C., Paul, A.M., Wake, C.P., 2003. A 154a high-resolution ammonium record from the Rongbuk Glacier, North slope of Mt. Qomolangma (Everest), Tibet-Himalaya region. *Atmos. Environ.* 37, 721–729. [https://doi.org/10.1016/S1352-2310\(02\)00582-4](https://doi.org/10.1016/S1352-2310(02)00582-4).
- Ikegami, K., Inoue, J., Higuchi, K., Ono, A., 2009. Atmospheric aerosol particles observed in high altitude Himalayas. *J. Jpn. Soc. Snow Ice* 40, 50–55. https://doi.org/10.5331/seppyo.40.Special_50.
- Jones, P.D., Parker, D., Osborn, T.J., Briffa, K.R., 2010. Global and hemispheric temperature anomalies—land and marine instrument records. In: Trends: A compendium of data on global change. Carbon Dioxide Information Analysis Center, <https://doi.org/10.3334/CDIAC/cli.002>. Oak Ridge National Laboratory, U.S. Department of Energy, Oak Ridge, Tenn., U.S.A.
- Joswiak, D.R., Yao, T., Wu, G., Xu, B., W., Z., 2010. A 70-yr record of oxygen-18 variability in an ice core from the Tanggula Mountains, central Tibetan Plateau. *Clim. Past* 6, 219–227. <https://doi.org/10.5194/cp-6-219-2010>.
- Kang, S.C., Mayewski, P.A., Qin, D., Yan, H., Hou, S., Zhang, D., Ren, J., Kruetz, K., 2002a. Glaciochemical records from a Mt. Everest ice core: relationship to atmospheric circulation over Asia. *Atmos. Environ.* 36, 3351–3361. [https://doi.org/10.1016/S1352-2310\(02\)00325-4](https://doi.org/10.1016/S1352-2310(02)00325-4).
- Kang, S.C., Mayewski, P.A., Qin, D.H., Yan, Y.P., Zhang, D.Q., Hou, S.G., Ren, J.W., 2002b. Twentieth century increase of atmospheric ammonia recorded in Mount Everest ice core. *J. Geophys. Res.* 107, 4595. <https://doi.org/10.1029/2001jd001413>.
- Kang, S.C., Wake, C.P., Qin, D.H., Mayewski, P.A., Yao, T.D., 2000. Monsoon and dust signals recorded in Dasuopu Glacier, Tibetan Plateau. *J. Glaciol.* 46, 222–226. <https://doi.org/10.3189/172756500781832864>.
- Kaufman, Y., Tanré, D., Boucher, O., 2002. A satellite view of aerosols in the climate system. *Nature* 419, 215–223. <https://doi.org/10.1038/nature01091>.
- Krotkov, N., McLinden, C., Li, C., Lamsal, L., Celarier, E., Marchenko, V., Swartz, S., Bucsela, W., Joanna, E., Duncan, J., Boersma, B., Pepijn, K., Veefkind, J., Levelt, P., Fioletov, V., Dickerson, R., He, H., Lu, Z., David, G., Streets, 2016. Aura OMI observations of regional SO₂ and NO₂ pollution changes from 2005 to 2015. *Atmos. Chem. Phys.* 16, 4605–4629. <https://doi.org/10.5194/acp-16-4605-2016>.
- Legrand, M.R., Delmas, R.J., 1986. Relative contribution of tropospheric and stratospheric sources to nitrate in Antarctic snow. *Tellus* 38B, 236–249. [https://doi.org/10.3402/tellus.\(v38\)i3.15132](https://doi.org/10.3402/tellus.(v38)i3.15132).
- Lelieveld, J., Bourtsoukidis, E., Brühl, C., Fischer, H., Fuchs, H., Harder, H., Hofzumahaus, A., Holland, F., Marno, D., Neumaier, M., Pozzer, A., Schlager, H., Williams, J., Zahn, A., Ziereis, H., 2018. The South Asian monsoon—pollution pump and purifier. *Science* 361<https://doi.org/10.1126/science.aar2501>. (ear2501).
- Liu, W.G., Ren, J.W., Qin, X., Liu, J.S., Kang, S.C., Cui, X.Q., Wang, Q., 2010. Hydrological characteristics of the Runoff Yield and Runoff confluence in the Rongbuk Glacier catchment in Mt. Qomolangma, Central Himalayas, China. *J. Glaciol. Geocryol.* 32, 367–372. <https://doi.org/10.1017/S0004972710001772>.
- Luo, R.S., Cao, J., Liu, G.N., Cui, Z.J., 2003. Characteristics of the subglacially-formed debris-rich chemical deposits and related subglacial processes of Qiangyong Glacier, Tibet. *J. Geogr. Sci.* 13, 455–462. <https://doi.org/10.1007/BF02837884>.
- Lüthi, Z.L., Škerlak, B., Kim, S.W., Lauer, A., Mues, A., Rupakheti, M., Kang, S., 2014. Atmospheric brown clouds reach the Tibetan Plateau by crossing the Himalayas. *Atmos. Chem. Phys.* 14, 6007–6021. <https://doi.org/10.5194/acpd-14-28105-2014>.
- Mayewski, P.A., Lyons, W.B., Ahmad, N., 1983. Chemical composition of a high altitude fresh snowfall in the Ladakh Himalayas. *Geophys. Res. Lett.* 10, 105–108. <https://doi.org/10.1029/GL010i001p00105>.
- Meeker, L.D., Mayewski, P.A., Twickler, M.S., Whitlow, S.I., Meese, D., 1997. A 110,000-year history of change in Continental biogenic emissions and related atmospheric circulation inferred from the Greenland Ice Sheet Project Ice Core. *J. Geophys. Res.* 102, 26489–26504. <https://doi.org/10.1029/97JC01492>.
- Pohjola, V.A., Moore, J.C., Isaksson, E., Jauhainen, T., Wal, R.S.W.V.D., Martma, T., Meijer, H.A.J., Vaikmäe, R., 2002. Effect of period melting on geochemical and isotopic signals in an ice core from Lomonosovfonna, Svalbard. *J. Geophys. Res. Atmos.* 107<https://doi.org/10.1029/2000JD000149>. (ACL-1-ACL 1-14).
- Qin, D.H., Hou, S.G., Zhang, D.Q., Ren, J.W., Kang, S.C., Mayewski, A.P., Wake, C.P., 2002. Preliminary results from the chemical records of an 80.4 m ice core recovered from East Rongbuk Glacier, Qomolangma (Mount Everest), Himalaya. *Ann. Glaciol.* 35, 278–284. <https://doi.org/10.3189/172756402781816799>.
- Rasmusson, E.M., Carpenter, T.H., 1982. Variations in Tropical sea surface temperature and surface wind fields associated with the Southern Oscillation/El Niño. *Mon. Weather. Rev.* 110, 354–384. [https://doi.org/10.1175/1520-0493\(1982\)110<354:VITSST>2.0.CO;2](https://doi.org/10.1175/1520-0493(1982)110<354:VITSST>2.0.CO;2).
- Reis, S., Pinder, R.W., Zhang, M., Lijie, G., Sutton, M.A., 2009. Reactive nitrogen in atmospheric emission inventories. *Atmos. Chem. Phys.* 9, 7657–7677. <https://doi.org/10.5194/acp-9-7657-2009>.
- Rolph, G., Stein, A., Stunder, B., 2017. Real-time environmental applications and display system: READY. *Environ. Model. Softw.* 95, 210–228. <https://doi.org/10.1016/j.envsoft.2017.06.025>.
- Ropelewski, C.F., Jones, P.D., 1987. An extension of the Tahiti-Darwin Southern Oscillation Index. *Mon. Weather. Rev.* 115, 2161–2165. [https://doi.org/10.1175/1520-0493\(1987\)115<2161:AEOTS>2.0.CO;2](https://doi.org/10.1175/1520-0493(1987)115<2161:AEOTS>2.0.CO;2).
- Russell, A., McGregor, G.R., 2010. Southern hemisphere atmospheric circulation: impacts on Antarctic climate and reconstructions from Antarctic ice core data. *Clim. Chang.* 99, 155–192. <https://doi.org/10.1007/s10584-009-9673-4>.
- Schumann, U., Huntrieser, H., 2007. The global lightning-induced nitrogen oxides source. *Atmos. Chem. Phys.* 7, 3823–3907. <https://doi.org/10.5194/acp-7-2623-2007>.
- Shao, L.L., Tian, L.D., Cai, Z.Y., Cui, J.P., Zhu, D.Y., Chen, Y.H., Palcsu, L., 2017. Driver of the interannual variations of isotope in ice core from the middle of Tibetan Plateau. *Atmos. Res.* 188, 48–54. <https://doi.org/10.1016/j.atmosres.2017.01.006>.
- Sheng, W.K., Yao, T.D., Li, Y.F., Deng, Y.S., Xie, C., 1996. Origins of NO₃⁻ in the Guliya Ice Cap. *J. Glaciol. Geocryol.* 18, 353–359.
- Shrestha, A.B., Wake, C.P., Dibb, J.E., 1997. Chemical composition of aerosol and snow in the high Himalaya during the summer monsoon season. *Atmos. Environ.* 31, 2815–2826. [https://doi.org/10.1016/S1352-2310\(97\)00047-2](https://doi.org/10.1016/S1352-2310(97)00047-2).
- Siegenthaler, U., Oeschger, H., 1980. Correlation of ¹⁸O in precipitation with temperature and altitude. *Nature* 285, 314–317. <https://doi.org/10.1038/285314a0>.
- Stein, A.F., Draxler, R.R., Rolph, G.D., Stunder, B.J.B., Cohen, M.D., Ngan, F., 2015. NOAA's Hysplit atmospheric transport and dispersion modeling system. *B. Am. Meteorol. Soc.* 96, 2059–2077. <https://doi.org/10.1175/Bams-D-14-00110.1>.
- Sun, S., Kang, S.C., Huang, J., Li, C., Guo, J., Zhang, Q., Sun, X., Tripathee, L., 2016. Distribution and transportation of mercury from glacier to lake in the Qiangyong Glacier Basin, Southern Tibetan Plateau, China. *J. Environ. Sci. (China)* 44, 213–223. <https://doi.org/10.1016/j.jes.2015.09.017>.
- Sutton, M.A., Reis, S., Riddick, S.N., Dragostis, U., Nemitz, E., Theobald, M.R., Tang, Y.S., Braban, C.F., Vieno, M., Dore, A.J., 2013. Towards a climate-dependent paradigm of ammonia emission and deposition. *Philos. Trans. R. Soc. B Biol. Sci.* 368, 20130166. <https://doi.org/10.1098/rstb.2013.0166>.
- Thompson, L., Yao, T.D., Thompson, E.M., Davis, M.E., Henderson, K.A., Lin, P., 2000. A high-resolution millennial record of the South Asian monsoon from Himalayan ice cores. *Science* 289, 1916–1919. <https://doi.org/10.1126/science.289.5486.1916>.
- Tian, L.D., Liu, Z.F., Gong, T.L., Yin, C.L., Yu, W.S., Yao, T.D., 2008. Isotopic variation in the lake water balance at the Yamdrok-iso basin, Southern Tibetan Plateau. *Hydrol. Process.* 22, 3386–3392. <https://doi.org/10.1002/hyp.6919>.
- Tian, L.D., Masson-Delmotte, V., Steinen, M., Yao, T.D., Jouzel, J., 2001. Tibetan Plateau summer monsoon northward extent revealed by measurements of water stable isotopes. *J. Geophys. Res.* 106, 28081–28088. <https://doi.org/10.1029/2001jd900186>.
- Tian, L.D., Yao, T.D., MacClune, K., White, J.W.C., Schilla, A., Vaughn, B., Vachon, R., Ichiyaniagi, K., 2007. Stable isotopic variations in West China: a consideration of moisture sources. *J. Geophys. Res.-Atmos.* 112, D10112. <https://doi.org/10.1029/2006JD007718>.
- Tian, L.D., Yao, T.D., Schuster, P.F., White, J.W.C., Ichiyaniagi, K., Pendall, E., Pu, J., Yu, W., 2003. Oxygen-18 concentrations in recent precipitation and ice cores on the Tibetan Plateau. *J. Geophys. Res.* 108<https://doi.org/10.1029/2002jd002173>. ACH 16-11-16-19.
- Tian, L.D., Yao, T.D., Wu, G.J., Li, Z., Xu, B.N., Li, Y.F., 2007. Chernobyl nuclear accident revealed from the 7010 m Muztagata ice core record. *Chin. Sci. Bull.* 52, 1436–1439. <https://doi.org/10.1007/s11434-007-0188-y>.
- GEO5 global environment outlook: environment for the future we want. In: UNEP (Ed.), UNEP.
- Vuille, M., Werner, M., Bradley, R.S., Keimig, F., 2005. Stable isotopes in precipitation in the Asian monsoon region. *J. Geophys. Res.* 110. <https://doi.org/10.1029/2005JD006022>.
- Wake, C.P., Mayewski, P.A., Wang, P., Yang, Q., Han, J., Xie, Z., 1992. Anthropogenic sulfate and Asian dust signals in snow from Tien Shan, Northwest China. *Ann. Glaciol.* 16, 45–52. <https://doi.org/10.3189/1992aog16-1-45-52>.
- Wake, C.P., Mayewski, P.A., Xie, Z.C., Wang, P., Li, Z.Q., 1993. Regional distribution of monsoon and desert dust signals recorded in Asian glaciers. *Geophys. Res. Lett.* 20, 1411–1414. <https://doi.org/10.1029/93GL01682>.
- Wang, Z.Y., Ma, Y.M., Liu, J.S., Han, C.B., 2013. Characteristic analyses on hydrological and related meteorological factors on the North Slope of Mount Qomolangma. *Plateau Meteorol.* 32, 31–37.
- Warneck, P., 1988. Chemistry of the Natural Atmosphere. International Geophysics 41. Academic Press Inc, Orlando FL, pp. 1–70. <https://doi.org/10.1126/science.152.3720.340>.
- Whetton, P., Rutherford, I., 1994. Historical ENSO teleconnections in the Eastern Hemisphere. *Clim. Chang.* 28, 221–253. <https://doi.org/10.1007/BF01104135>.
- Xu, M., Kang, S.C., Wu, H., Yuan, X., 2018. Detection of spatio-temporal variability of air temperature and precipitation based on long-term meteorological station observations over Tianshan Mountains, Central Asia. *Atmos. Res.* 203, 141–163. <https://doi.org/10.1016/j.atmosres.2017.12.007>.
- Yamaji, K., Ohara, T., Akimoto, H., 2004. Regional-specific emission inventory for NH₃, N₂O, and CH₄ via animal farming in South, Southeast, and East Asia. *Atmos. Environ.* 38, 7111–7121. <https://doi.org/10.1016/j.atmosenv.2004.06.045>.
- Yan, X.Y., Akimoto, H., Ohara, T., 2003. Estimation of nitrous oxide, nitric oxide and ammonia emissions from croplands in East, Southeast and South Asia. *Glob. Chang. Biol.* 9, 1080–1096. <https://doi.org/10.1046/j.1365-2486.2003.00649.x>.
- Yang, J.P., Tan, C.P., Zhang, T.J., 2012. Spatial and temporal variations in air temperature and precipitation in the Chinese Himalayas during the 1971–2007. *Int. J. Climatol.* 33, 2622–2632. <https://doi.org/10.1002/joc.3609>.

- Yao, T.D., Masson, V., Jouzel, J., Steinenard, M., Sun, W.Z., Jiao, K.Q., 1999. Relationships between $\delta^{18}\text{O}$ in precipitation and surface air temperature in the Urumqi River Basin, east Tianshan Mountains, China. *Geophys. Res. Lett.* 26, 3473–3476. <https://doi.org/10.1029/1999GL006061>.
- Yao, T.D., Masson-Delmotte, V., Gao, J., Yu, W.S., Yang, X.X., Risi, C., Sturm, C., Werner, M., Zhao, H.B., He, Y., Ren, W., Tian, L.D., Shi, C.M., Hou, S.G., 2013. A review of climatic controls on $\delta^{18}\text{O}$ in precipitation over the Tibetan Plateau: observations and simulations. *Rev. Geophys.* 51, 525–548. <https://doi.org/10.1002/rog.20023>.
- Ye, Q.H., Zhu, L.P., Zheng, H.X., Naruse, R., Zhang, X.Q., Kang, S.C., 2017. Glacier and lake variations in the Yamzhog Yumco basin, southern Tibetan Plateau, from 1980 to 2000 using remote-sensing and GIS technologies. *J. Glaciol.* 53, 673–676. <https://doi.org/10.3189/002214307784409261>.
- Zhang, Q.G., Kang, S.C., Kaspari, S., Li, C.L., Qin, D.H., Mayewski, P.A., Hou, S.G., 2009. Rare earth elements in an ice core from Mt. Everest: seasonal variations and potential sources. *Atmos. Res.* 94, 300–312. <https://doi.org/10.1016/j.atmosres.2009.06.005>.
- Zhang, Y.L., Kang, S.C., Zhang, Q.G., Grigholm, B., Kaspari, S., You, Q.L., Qin, D.H., Mayewski, P.A., Cong, Z.Y., Huang, J., Sillanpää, M., Chen, F., 2015. A 500 year atmospheric dust deposition retrieved from a Mt. Geladaindong ice core in the central Tibetan Plateau. *Atmos. Res.* 166, 1–9. <https://doi.org/10.1016/j.atmosres.2015.06.007>.
- Zhao, H.B., Yao, T.D., Xu, B.Q., Li, Z., Duan, K.Q., 2008. Ammonium record over the last 96 years from the Muztagata glacier in Central Asia. *Chin. Sci. Bull.* 53, 1255–1261. <https://doi.org/10.1007/s11434-008-0139-2>.
- Zheng, W., Yao, T.D., Joswiak, D.R., Xu, B.Q., Wang, N.L., Zhao, H.B., 2010. Major ions composition records from a shallow ice core on Mt. Tanggula in the Central Qinghai-Tibetan Plateau. *Atmos. Res.* 97, 70–79. <https://doi.org/10.1016/j.atmosres.2010.03.008>.